# ALTOS

## Managing water resources within Mediterranean agrosystems by accounting for spatial structures and connectivities.

WP1 aims to characterize spatial structures and connectivities by developing innovating tools for observation and numerical representation:

- The **spatial structures** at local- and landscape- scales are:

(1) natural structures related to vegetation, soils, water resources and climate, as well as (2) anthropogenic structures such as landscaping features and agricultural practices.

- The **hydrological connectivities** are surface and subsurface connections between elements.

***"Innovative methodologies rely on the joint use of complementary observations with high spatio-temporal resolutions, as well as on typology based segmentations or deep learning-based processing of multisource information".***

## Task 1.1: Object geometries and landscape structures

- Canopy
- Aquifers
- Soils
- Infiltrability
- Climate variability

## Task 1.1: Object geometries and landscape structures

- Canopy

**Accurate estimates of canopy transpiration (i.e. energy balance models or crop modelling) needs an accurate characterization of the structural & biophysical parameters of the vegetation: LAI, FAPAR, FVC ...**

**To improve the estimates of structural & biophysical parameters of the vegetation through novel Remote Sensing approaches**

# Study 1.

- Photogrammetry
- Spectral vegetation índices (VI)
- Radiative Transfer Models (RTM)

→ FIPAR

LAI


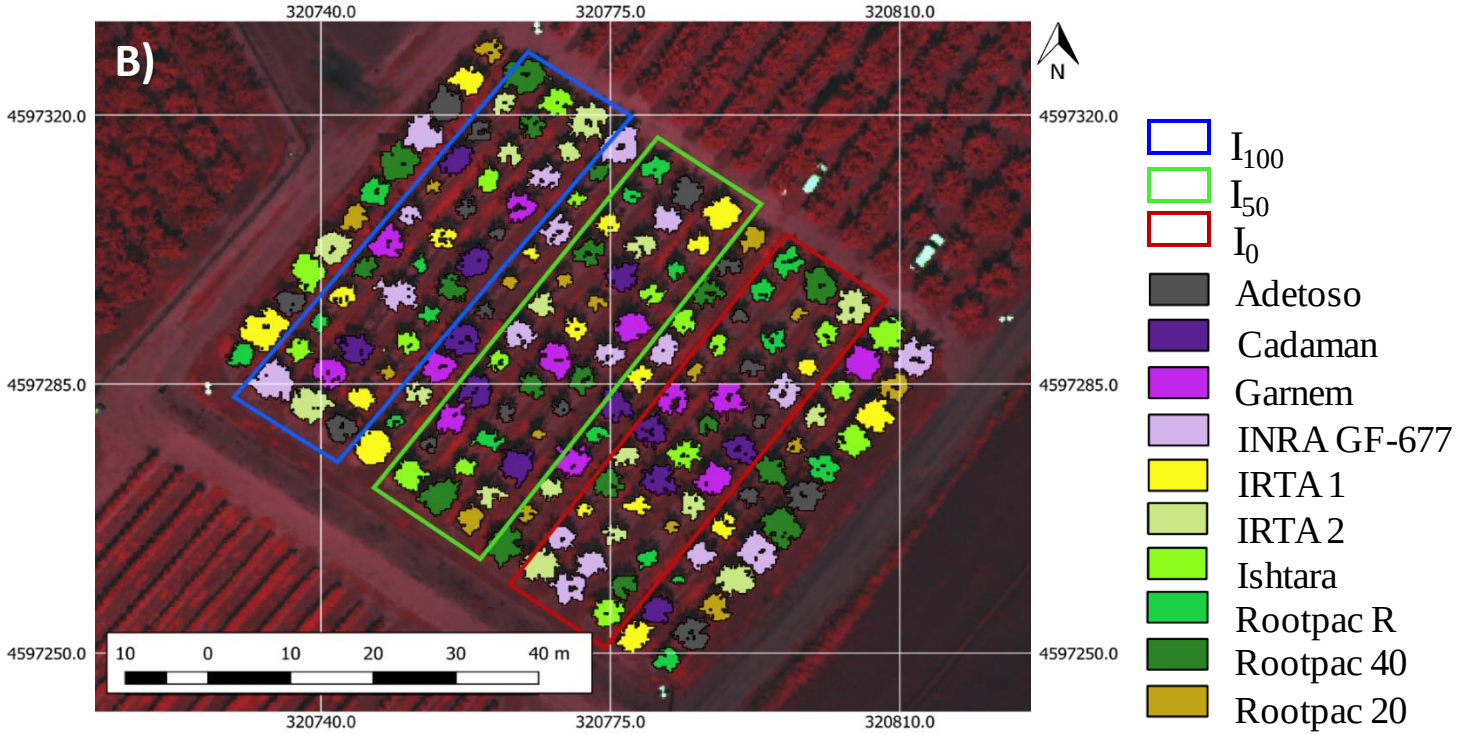


*Bellvert et al. (2021) Frontiers in Plant Science*

# Photogrammetry

# Photogrammetry

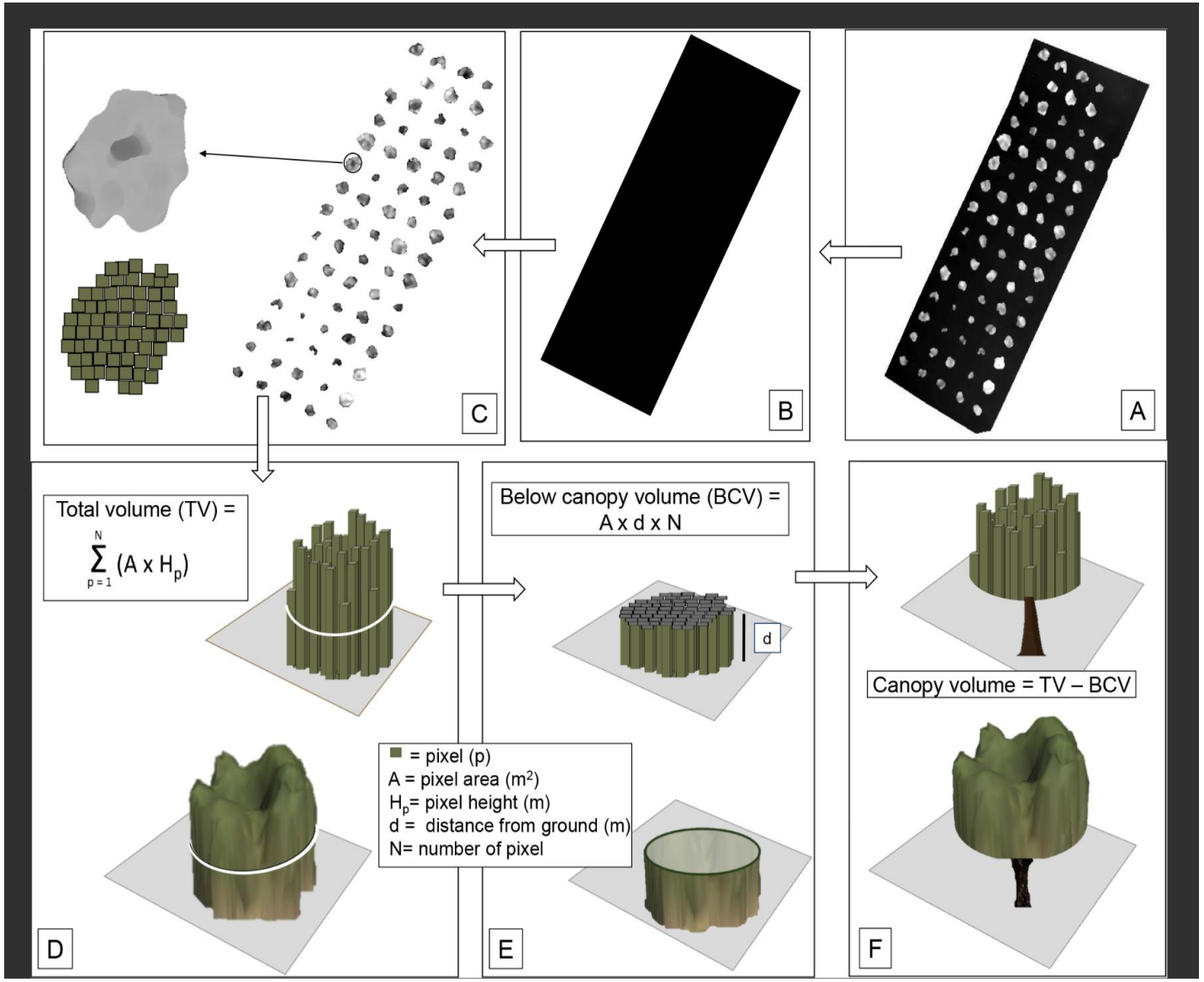


-> Crown Area ($m^2$)
-> Canopy Height
-> Total canopy volumen ($m^3$)

## Spectral Vegetation Indices

**TABLE 2** List of spectral vegetation indices (VI), their formulation and reference. *R* is defined as reflectance.

| Index | Formula | Reference |
|---|---|---|
| NDVI | $(R_{870}-R_{680})/(R_{870}+R_{680})$ | Rouset et al. (1973) |
| GNDVI | $(R_{870}-R_{570})/(R_{870}+R_{570})$ | Gitelson et al. (1998) |
| MCARI | $[(R_{710}-R_{680})-0.2(R_{710}-R_{570})]\ R_{710}/R_{680}$ | Daughtry et al. (2000) |
| NDRE | $(R_{870}-R_{710})/(R_{870}+R_{710})$ | Barnes et al. (2000) |
| MSRRE | $(R_{870}/R_{710})-1/\sqrt{R_{870}+R_{710}+1}$ | Wu et al. (2008) |

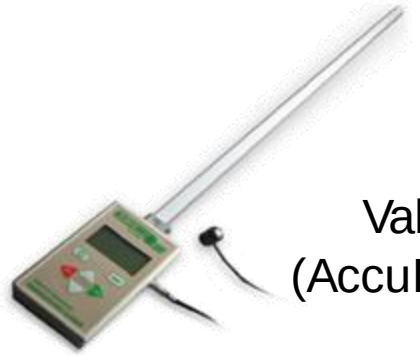

Validations
(AccuPAR LP-80)

## MACAW TetraCam (6 bands)

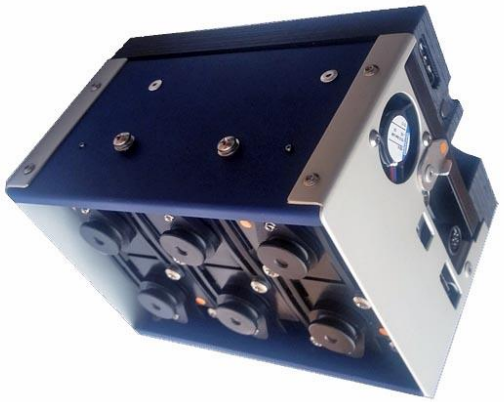

## Radiative Transfer Models

**TABLE 3.** List of parameters and their ranges used in PROSAIL reflectance modeling.

| Image Acquisition | 24th July 2018 | 28th August 2018 | 24th July 2019 |
|---|---|---|---|
| DOY | 205 | 240 | 205 |
| Time image acquisition | 12.50 | 12.25 | 12.25 |
| Solar irradiance ($W.m^{-2}$) | 924 | 778 | 910 |
| Solar zenith angle (°) | 21.81 | 32.04 | 21.38 |
| Solar azimuth angle (°) | 193.43 | 184.53 | 183.91 |
| Spectral bands (nm) | 515.3, 570.9, 682.2, 710.5, 781.1, 871.8 | | |
| Soil reflectance | 0.121, 0.163, 0.192, 0.319, 0.373, 0.363 | | |
| Number of simulations | 100000 | | |
| Latitude | 41.5 | | |
| Longitude | 0.85 | | |
| $N_{leaf}$ | 1.2-2.2 | | |
| $C_{ab}$ ($\mu g.cm^{-2}$) | 0-90 | | |
| $C_{ar}$ ($\mu g.cm^{-2}$) | 0-40 | | |
| $C_{brown}$ | 0.0-1.0 | | |
| $C_w$ ($g.cm^{-2}$) | 0.003-0.011 | | |
| $C_{dm}$ ($g.cm^{-2}$) | 0.003-0.011 | | |
| LAI | 0.0-6.0 | | |
| Average leaf angle (°) | 30-80 | | |
| Hotspot ($m.m^{-1}$) | 0.1-0.5 | | |

**TABLE 4.** Coefficients of determination ($R^2$) of the regressions between leaf area index (LAI) and daily fraction of intercepted radiation ($fiPAR_d$) with spectral vegetation indices (VIs), crown area and canopy volume, PROSAIL radiative transfer model, and multiple regression analysis with empirical variables.

| Parameters | NDVI | GNDVI | MCARI | NDRE | MSRre | Crown area ($m^2$) | Canopy volume ($m^3$) | Predicted LAI and *fiPAR* (PROSAIL) | Multiple regression analysis |
|---|---|---|---|---|---|---|---|---|---|
| **LAI** $_{24/7/2018}$ | 0.24 | 0.25 | 0.30 | 0.56 | 0.54 | 0.72 | 0.72 | y=0.45x+0.60, $R^2$=0.67, RMSE=0.24 | y=-0.74+3.31NDRE+0.03Volume, $R^2$=0.74, RMSE=0.19 |
| **LAI** $_{28/8/2018}$ | 0.57 | 0.50 | 0.49 | 0.51 | 0.48 | 0.65 | 0.64 | y=0.57x+0.20, $R^2$=0.46, RMSE=0.38 | y=-1.81+6.93GNDVI-1.98MSRre+0.02Volume, $R^2$=0.70, RMSE=0.17 |
| **LAI** $_{24/7/2019}$ | 0.41 | 0.41 | 0.36 | 0.42 | 0.41 | 0.44 | 0.49 | y=1.00x+0.05, $R^2$=0.56, RMSE=0.39 | y=-1.22+3.50NDRE+0.02Volume, $R^2$=0.54, RMSE=0.30 |
| **LAI** $_{all}$ | ns | ns | ns | 0.15 | ns | 0.59 | 0.58 | y=0.59x+0.49, $R^2$=0.40, RMSE=0.34 | y=0.49+1.98NDRE-1.06NDVI+0.03Volume, $R^2$=0.60, RMSE=0.24 |
| $fiPAR_{d\ 24/7/2018}$ | 0.37 | 0.39 | 0.15 | 0.49 | 0.46 | 0.53 | 0.50 | y=0.54x+0.28, $R^2$=0.64, RMSE=0.07 | y=-0.91+0.05MSRre+2.22NDVI+0.01Volume, $R^2$=0.64, RMSE=0.06 |
| $fiPAR_{d\ 28/8/2018}$ | 0.45 | 0.49 | 0.38 | 0.47 | 0.46 | 0.49 | 0.45 | y=0.80x+0.09, $R^2$=0.45, RMSE=0.14 | y=0.03+0.83GNDVI+0.01Volume, $R^2$=0.56, RMSE=0.05 |
| $fiPAR_{d\ 24/7/2019}$ | 0.38 | 0.40 | 0.32 | 0.41 | 0.39 | 0.38 | 0.43 | y=1.15x-0.15, $R^2$=0.51, RMSE=0.14 | y=-2.93-3.21MSRre+12.75NDRE, $R^2$=0.53, RMSE=0.10 |
| $fiPAR_{d\ all}$ | ns | 0.18 | ns | 0.16 | ns | 0.49 | 0.48 | y=0.44x+0.34, $R^2$=0.29, RMSE=0.12 | y=-0.24+0.62GNDVI+6.95MCARI+1.19NDRE-0.65NDVI+0.01Volume, $R^2$=0.56, RMSE=0.07 |

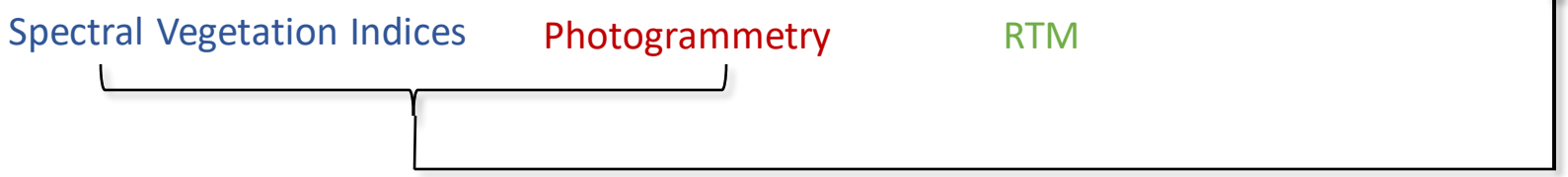


*Bellvert et al. (2021) Frontiers in Plant Science*

# Assessment of differences in water use efficiency between rootstocks

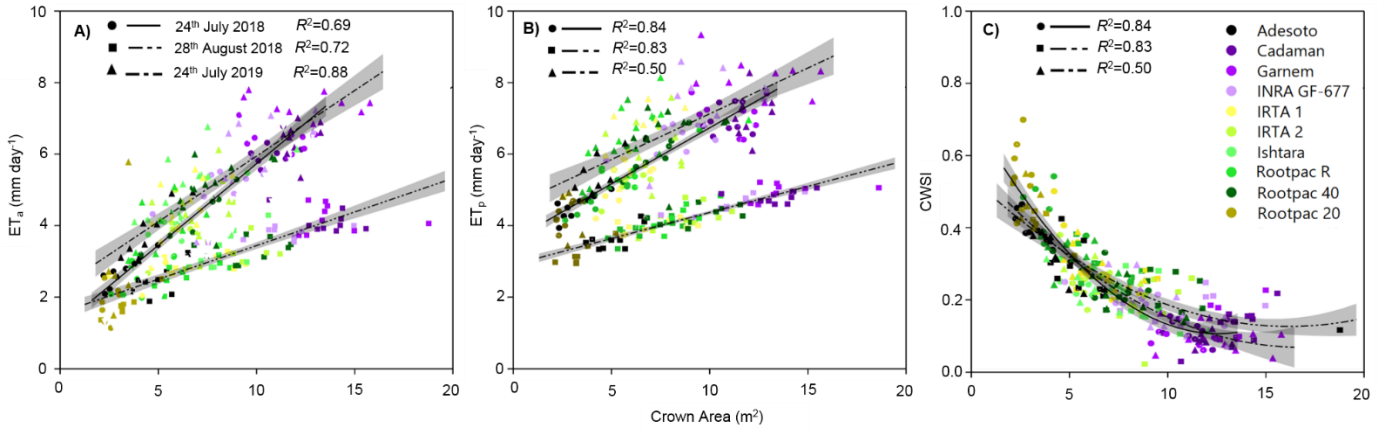


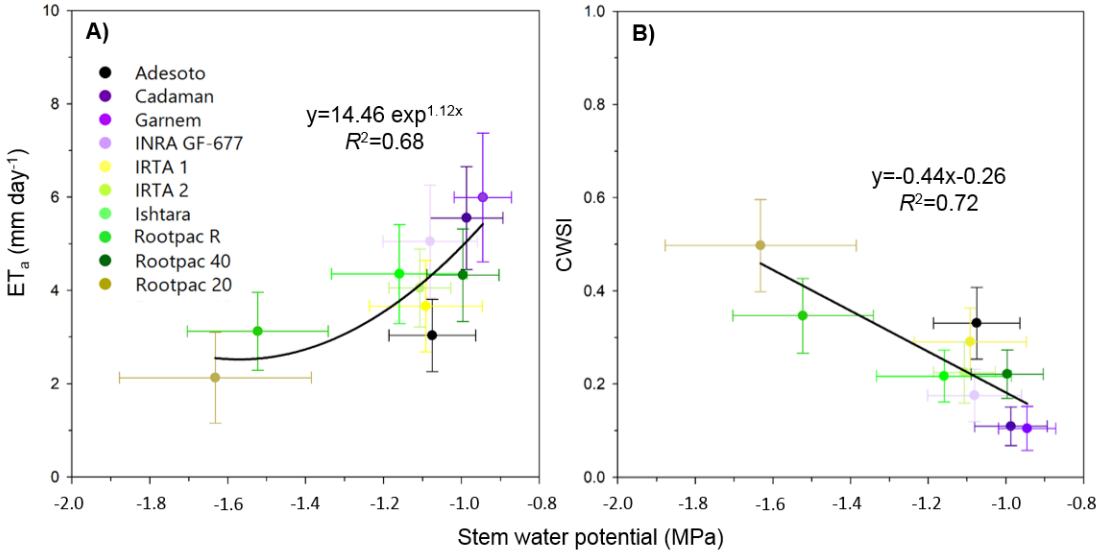


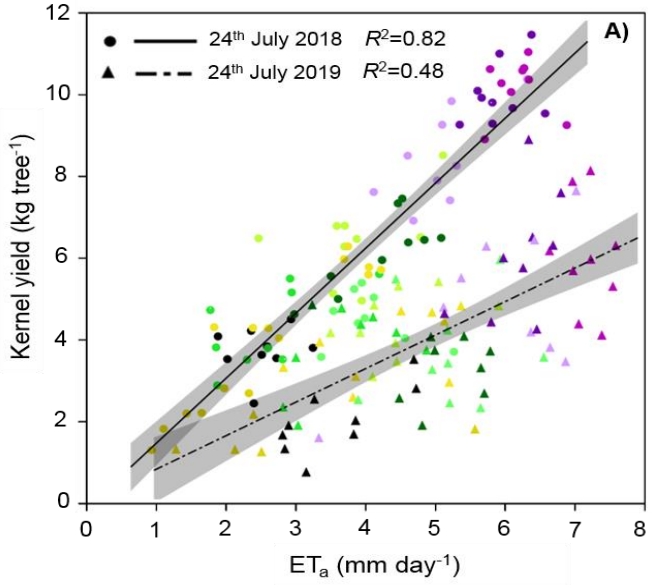


*Bellvert et al. (2021) Frontiers in Plant Science*

# **Study 2.** Almond trial (2021-2022)

**4 Training Systems vs. 3 Irrigation Treatments**

**1.** To compare different ‘point cloud’ techniques to estimate LAI and FIPAR: Terrestrial LIDAR vs. Photogrammetry.
**2.** Relate FIPAR and LAI with Transpiration (sap-flows)
**3.** To validate ET partitioning using TSEB model (very high-resolution imagery) against sap-flows
**4.** Obtain the water production functions (kg / $m^3$ water transpired)

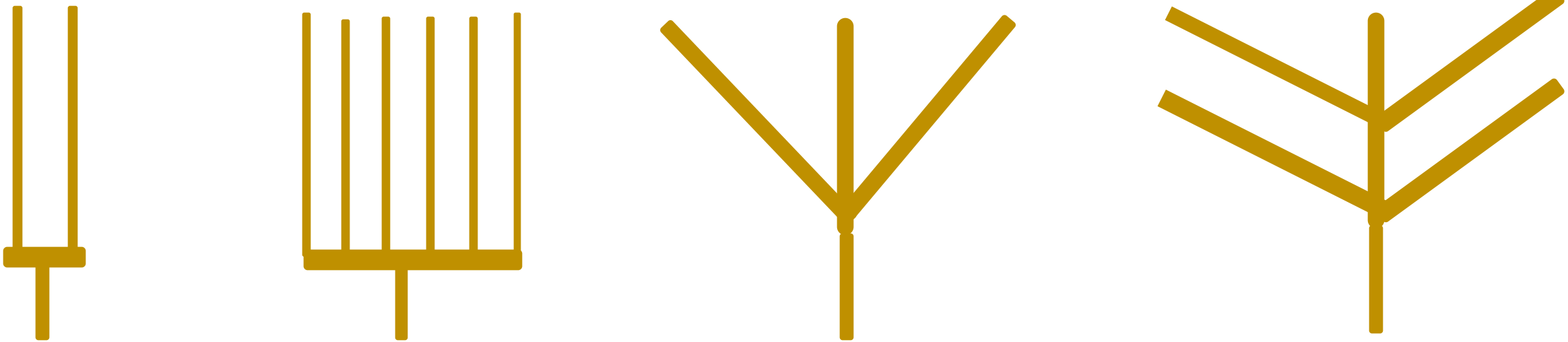

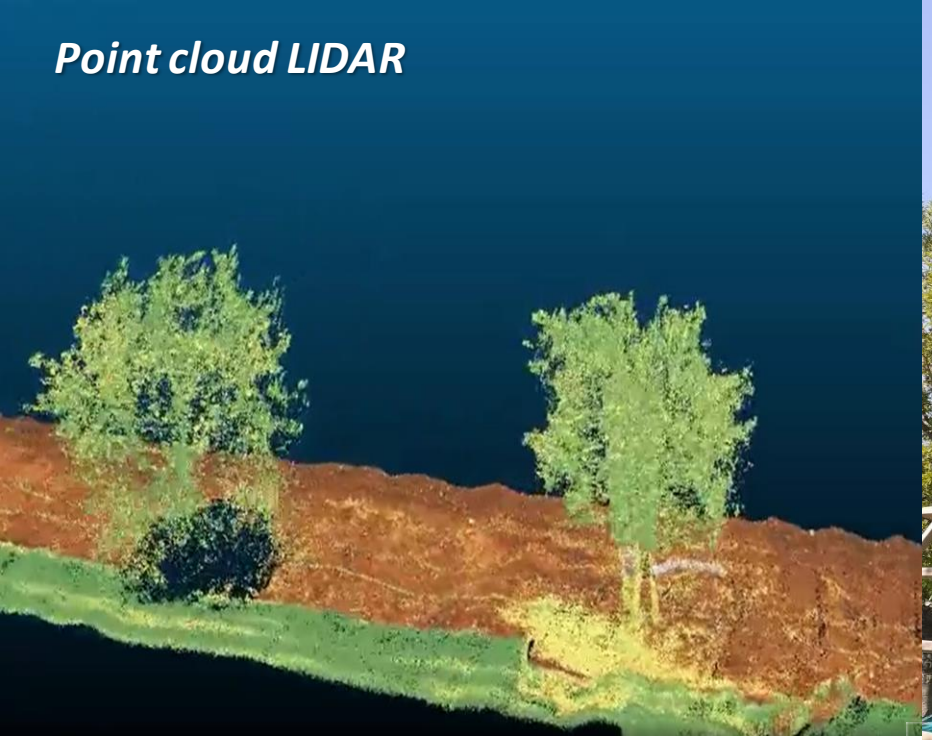


Validations

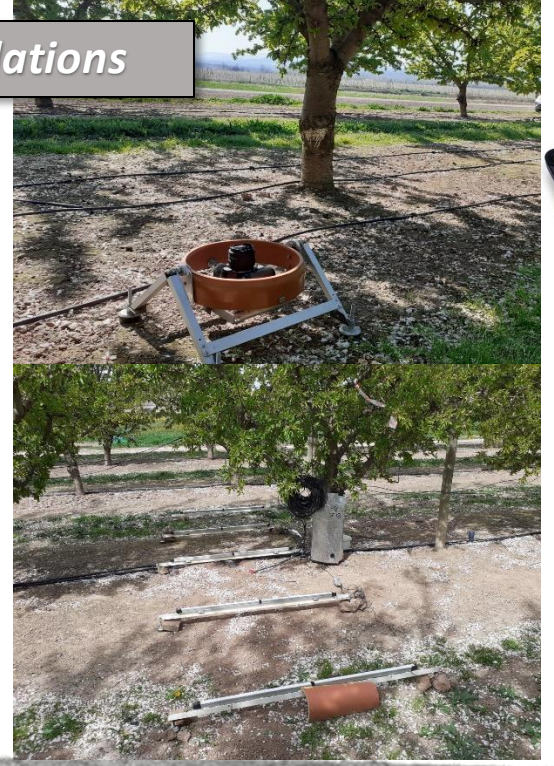

IRTA
RESEARCH & TECHNOLOGY
FOOD & AGRICULTURE


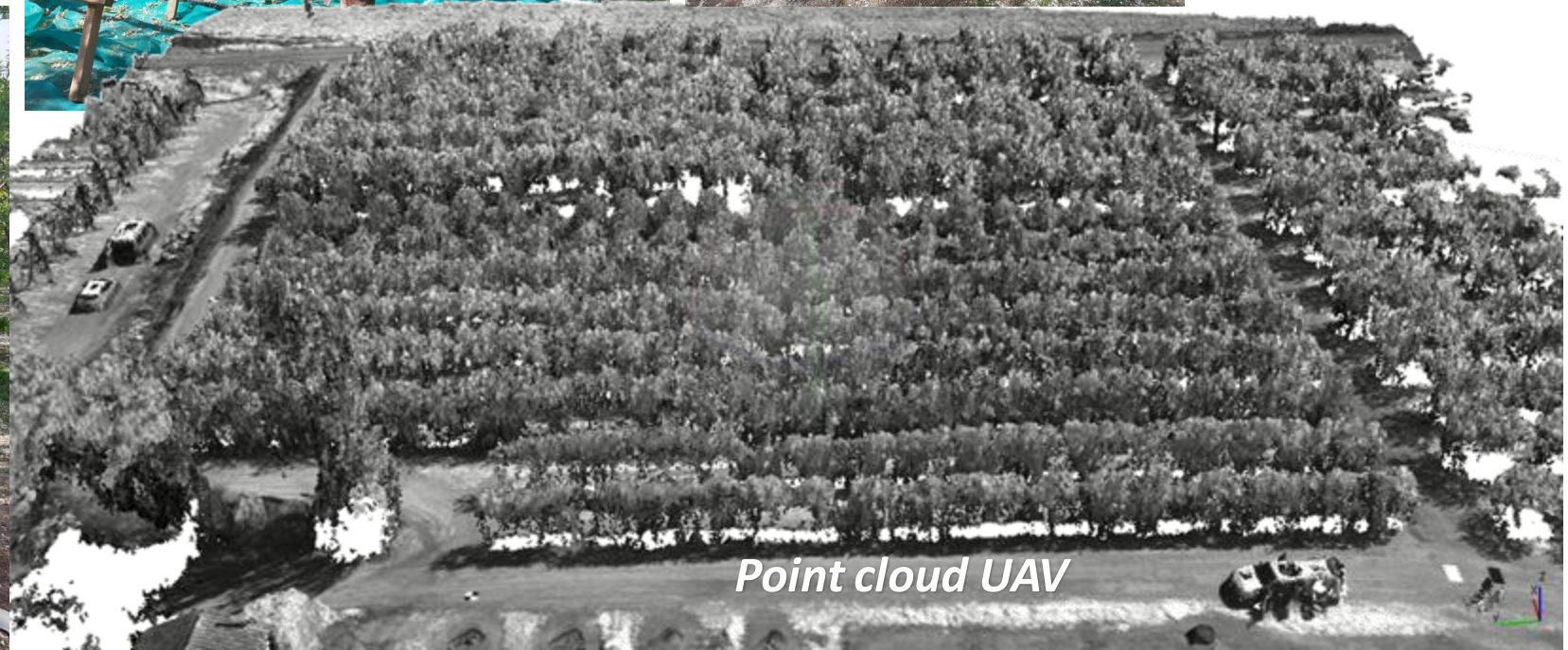

## Task 1.1: Object geometries and landscape structures

- Canopy

o Targets: density, height and roughness, crown size, row spacing / direction, profiles of fraction cover and leaf area index.

**-> need of LiDAR measurements for accurate olive tree crown for DART mock-up**

o Methodological innovations: 3D radiative transfer modelling with joint use of multispectral airborne data and Sentinel-1 & 2 satellite data, photogrammetric processing of multispectral airborne data.

**-> DART modelling to explain PRI measurements over olive tree**

**-> low cost TIR imagery over vineyard (Spain, installed) and Taous olive tree (to be installed in June 2021)**

Flux station at Verdú (CAT)
Drip irrigated vineyard 04/21-10-21
ESA WineEO, ANR Hiliaise, CNES TRISHNA projects.

# Task 1.1: Object geometries and landscape structures

PhD
Nejmeddine
OUHICHI

## • Aquifers

Targets: 3D description of aquifer structure and flow pathways. o Methodological innovations: joint use of geo-electrical methods, electromagnetic sounding, and stable isotopes (δ18O and δ2H). Partners: CERTE, UNICA.

### Objectives

- Aquifer structure characterization around Lebna dam (Geometry, and lithology)
- Leakage delineation
- Flow pathways

### Work performed

- Geological investigation; outcrop mapping,
- Lithological cross sections,
- Geophysics investigations:

  67 SEVs
  14 Tomography
  1 drilling well 30m for calibration
  6 Piezometrics surveys (71 boreholes)

- Piezometric mapping and monitoring

  Installation of 13 piezometric sensors;
  Installation of 6 Pezometers (of 3 to 7m deep);
  Topographic leveling (PZ, Boreholes and VES)

### Calendar & Difficulties: 2019-2021

Geophysics calibration
Only 1 drilling well 30m

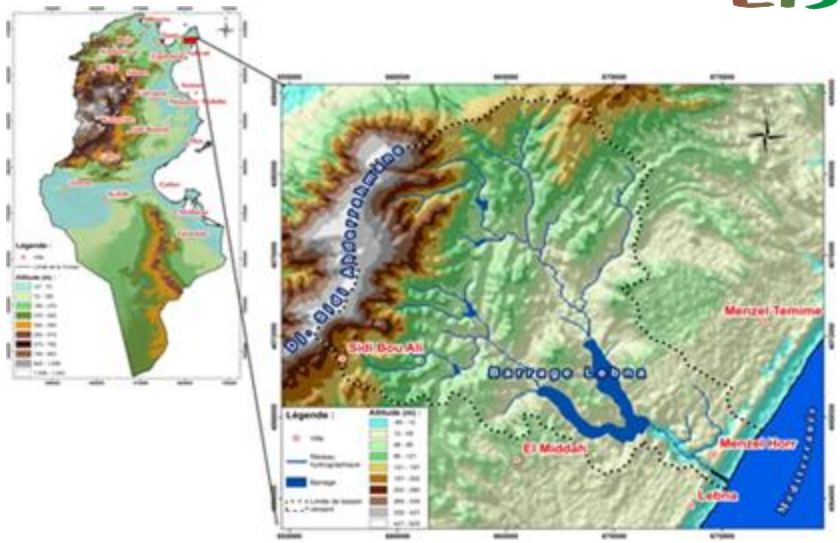


***Study area situation***

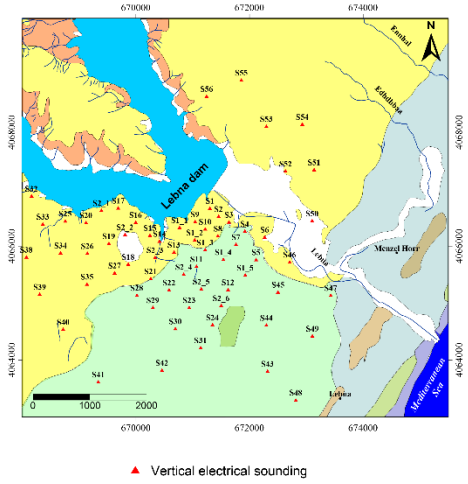


***Geophysics acquisition***

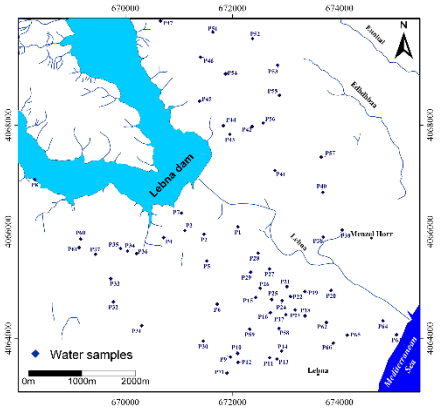


***Piezometric monitoring:***
***Positions of the 71 Water wells sampled***

PhD
Nejmeddine
OUHICHI

- **Aquifers**

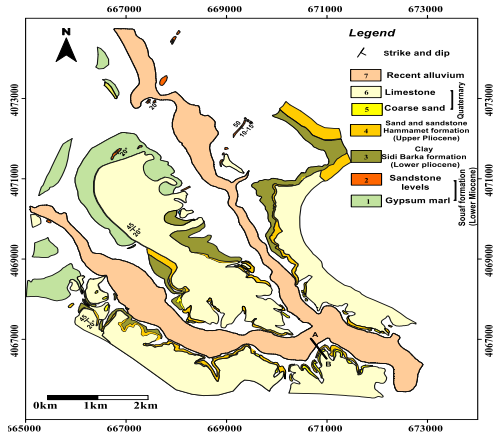


Geologic Mapping of the Lebna basin

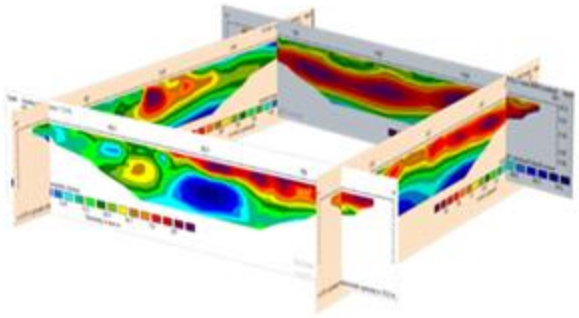

3D resistivity Diagram

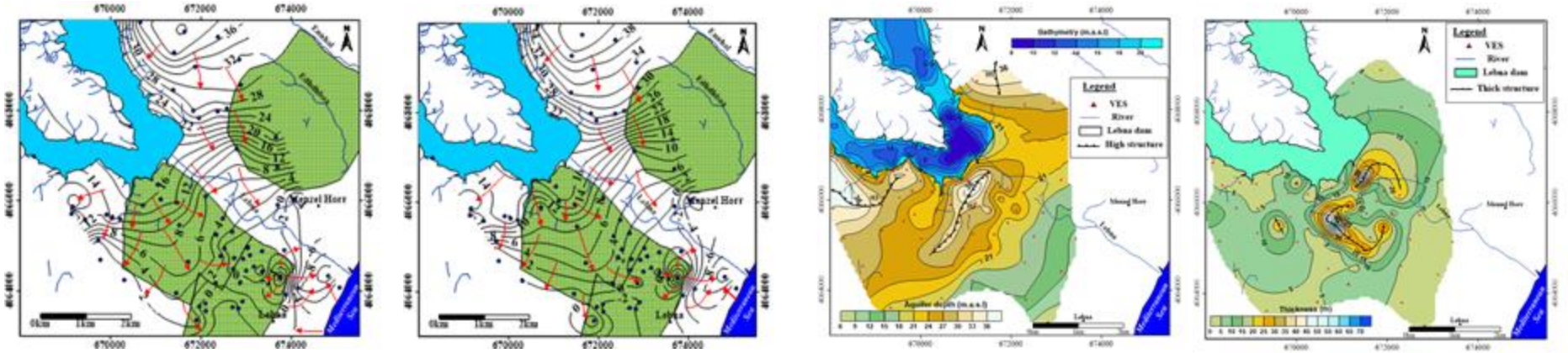

Coastal aquifer Piezometric maps : (a) in Feb.2020, (b) in August 2020



Isobath map of Lebna shallow aquifer



Isopach map of Lebna shallow aquifer

## To be done

- PS Geophysical investigation (CERTE/UNICA/LISAH)
- Piezometric maps of August and Feb 2021 and 2022

**Deliverables**

D1.1.1 [Task 1.1]: dataset @ Month 15

UNICA

## Task 1.1: Object geometries and landscape structures

### Activities

Soils and Aquifer:

-Geoelectrical methodologies for the description of aquifer structure and the definition of soil structure;

-Use of radar satellite data for the evaluation of soil moisture content;

-use of optical satellite data for Evapotranspiration estimate in a Sardinian Basin (in cooperation with CESBIO: a student from UNICA spent 3 months in CESBIO Lab);

UNICA

## -> Geoelectrical/geophysical methodologies for the description of aquifer structure and the definition of soil structure;

1. **Development of "novel" strategies for the characterization of the static and dynamic components of the subsurface:**

   1.1 new 4D algorithms for the inversion of time-lapse Electrical Resistivity Tomography (potentially, also, Induced Polarization) data.

   1.2 collection of 1 (before ALTOS) +2 (during Dec. 2020, Jan. 2021) + 1 (Jan. 2021 for calibration/validation of a new really-3D acquisition system – 256 channels) datasets on the Orroli's test site

   1.3 preliminary tests for a new ERT "permanent" 256-channel system

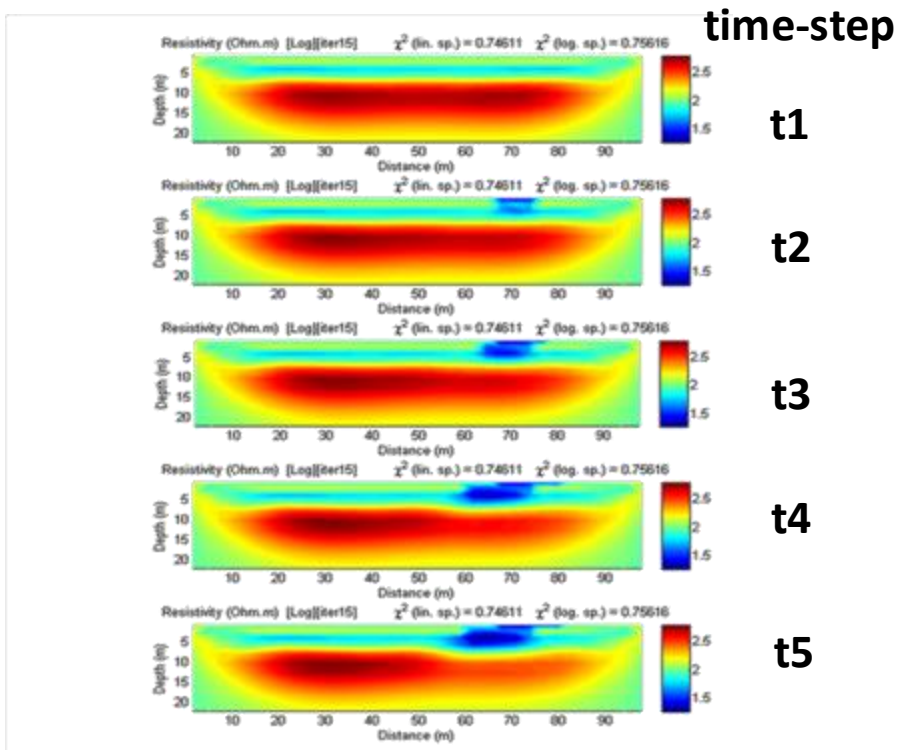


2. **Organization of a preliminary meeting between CERTE/UNICA/LISAH concerning the geophysical and remote- and proximal-sensing methodologies among the different sites of the project: Lebna (leaking dam) -Tunisia; Orroli (wild olive trees) – Italy; but, in case, also, Sfax (olive orchard – to be further discussed) – Tunisia**

   2.1 interesting data are available or are going to be available on all the sites. In particular besides the "standard" ERT data, at least for the Lebna and Orroli cases, the acquisition of Self-Potential (SP) measurements is planned.
   In fact, SP data might highlight the fluid movements (clearly crucial, for studying the leaking of the dam and the dynamics of the wild olive trees – in this second case, especially, if correlated with sap-flow and evapotranspiration measurements).

   2.2 the data will be exchanged between partners in order to more efficiently test the algorithms developed by one of the partners and to get the best out of each dataset.
   Sharing data and procedures, not only will optimize the resources, but will also foster mutual capacity-building and collaboration (to be implemented also via shared scientific publications).

   2.3 together with geoelectrical measurements, acquisition of other proximal-sensing data could be performed (e.g. electromagnetic induction, EMI, measurements). Also in this case, data and procedures for the data elaboration can be shared. If the pandemic situation will allow it, joint field campaigns (sharing also instrumentation) can be arranged in late 2021.

   2.4 the (time-lapse) geoelectrical/EMI data can be integrated with the remote-sensing measurements. This, potentially, could pave the road to the data-informed spatial extrapolation of proximal/geophysical results (more logistically expensive, but with a larger depth of investigation, DOI) via the remote-sensing observations (with a shallower DOI, but ubiquitous).

- **Spatial variability in soil infiltrability**

# 1/ mapping of soil surface characteristics related to soil infiltrability

Spatial characterization of the hydraulic conductivity of the upstream part of the Merguellil watershed in order to improve the hydrological characterization of the site and improving modelling results mainly of the SWAT model

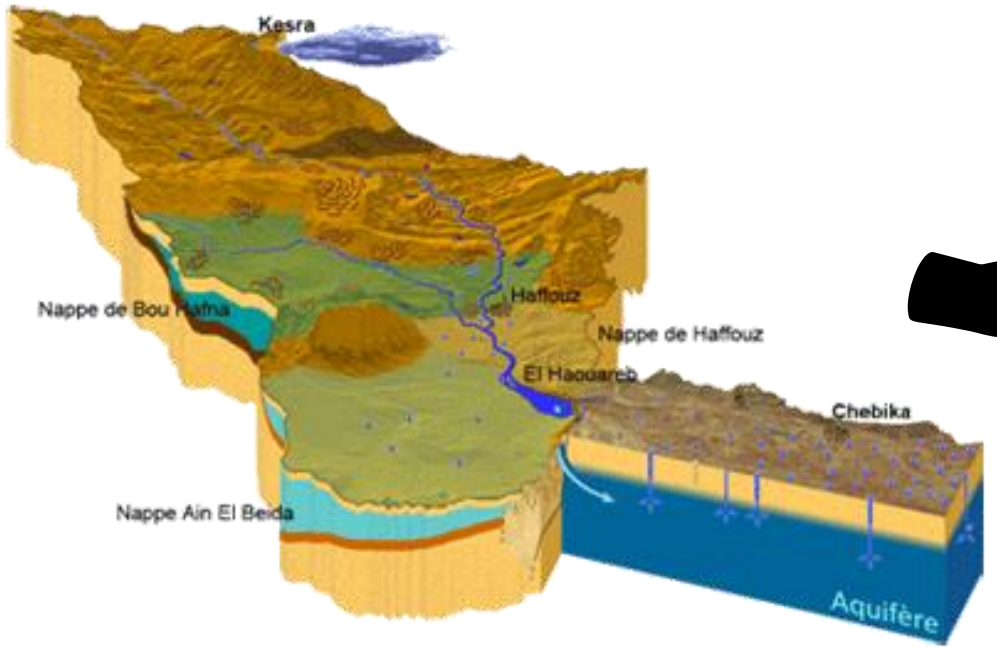


1

On site determination of the saturated hydraulic conductivity using the pressure infiltrometer

2

Using geostatistical method for the spatial distribution of the saturated hydraulic conductivity

- **Spatial variability in soil infiltrability**

## 2/ Methodological innovations: joint use of time series of optical and microwave remote sensing

* Use remotely sensed near-surface moisture from a passive microwave sensor for estimating the soil surface infiltrability
* The spatial and temporal variability of soil infiltration maps generated by remote sensing will be compared to the ground observations within the watershed

## Task 1.1: Object geometries and landscape structures

- Infiltrability

# Sentinel-2 images to assess soil surface characteristics over a rainfed Mediterranean cropping system

# Soil infiltration characteristics linked to soil surface characteristics

Results from works done over fields of ORE OMERE along 6 years

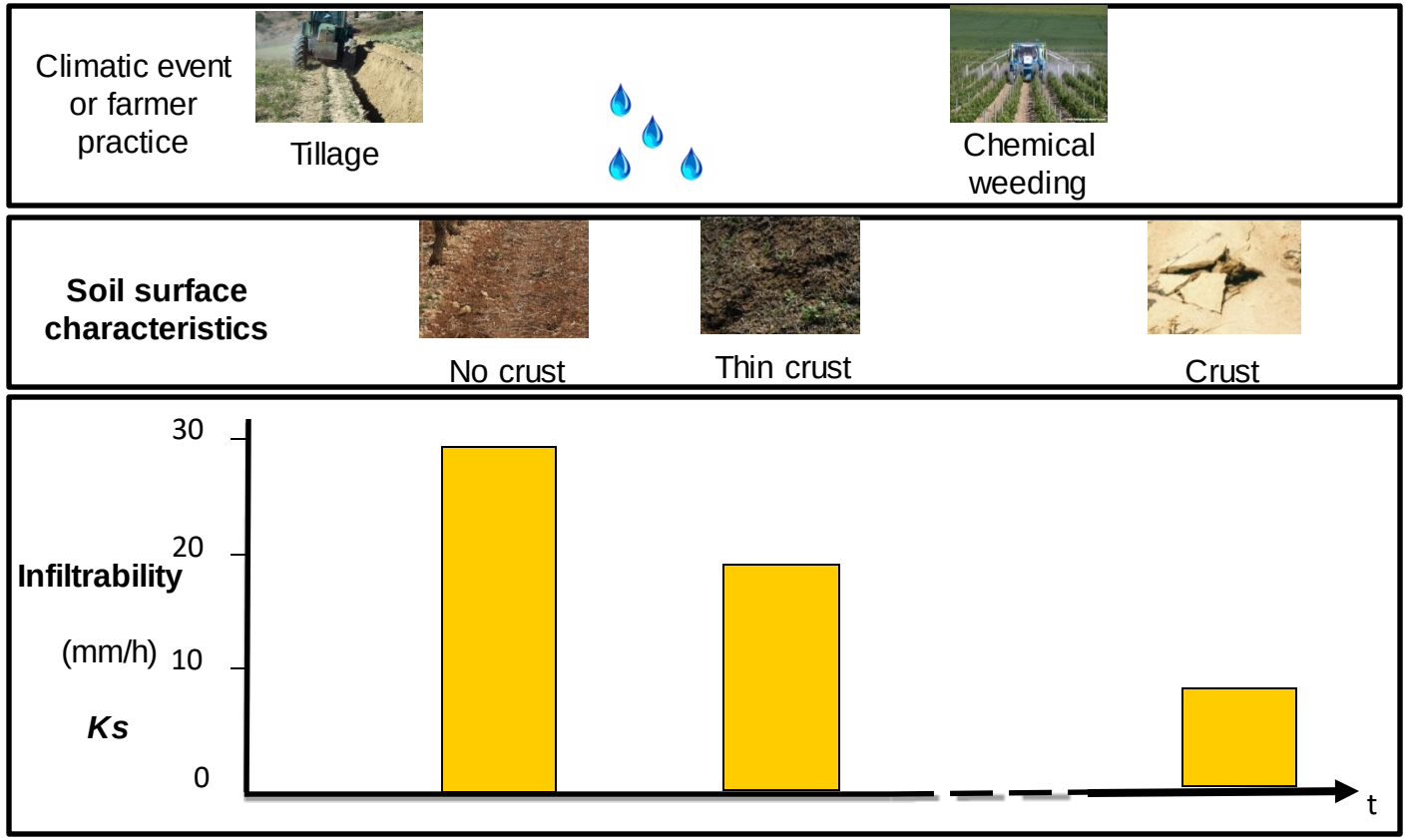


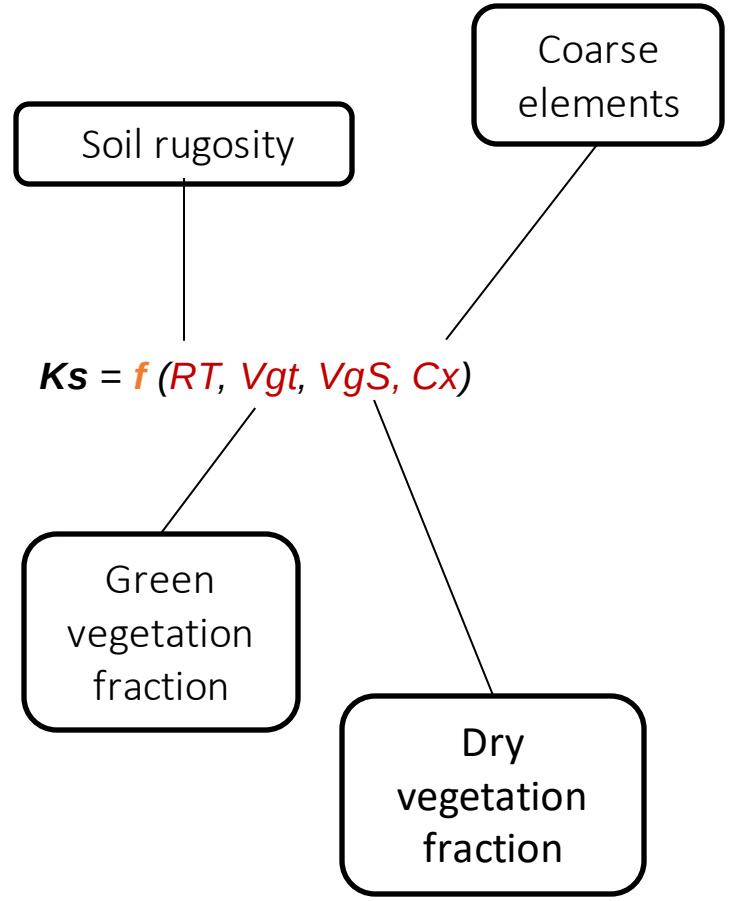


Can we monitor the soil surface characteristics (SSCs) (in space and time) ?

# Study Area

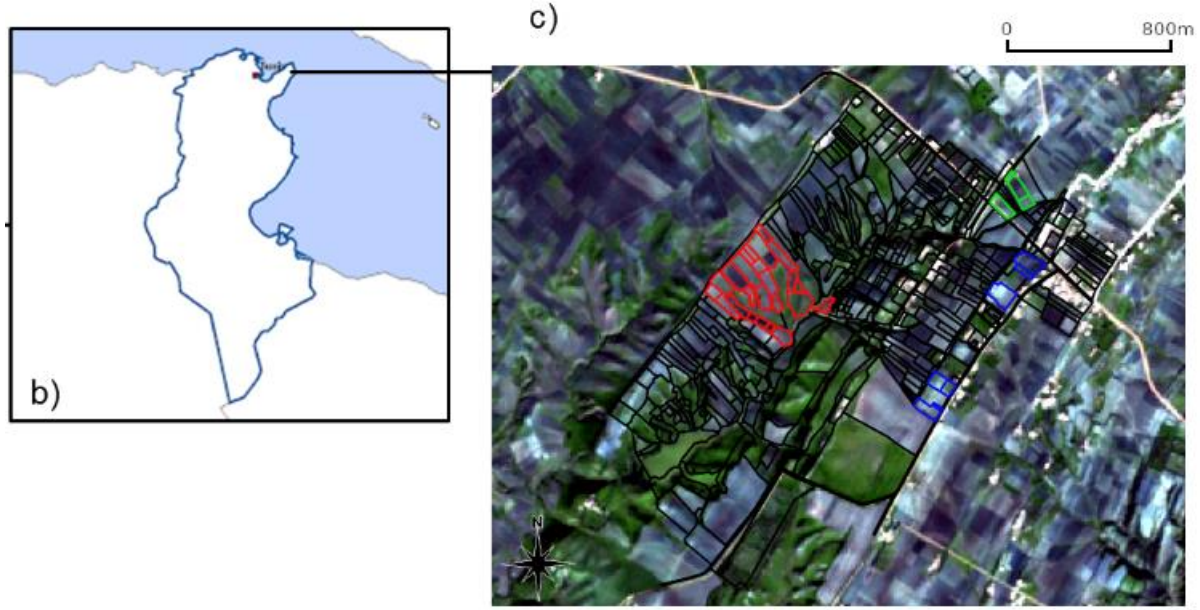


- Kamech catchment (2,63km²)
- 384 fields (mean plot area = 0,59 ha)
- SSCs observed over 34 fields, every 2 weeks (in red, blue, green on Figure c) :

# Field and satellite data

- SSCs studied:
  - *green vegetation fraction*
  - *dry vegetation fraction*
  - *physical soil surface structure*
- 5 sentinel-2 data (10 bands, 10 m resolution).
- Field boundaries map

| Date of S2 images acquisition (Y-M-D) | Date of field observations (Y-M-D) | Number of days between images acquisition and field observation |
|---|---|---|
| 2016-08-04 | 2016-09-01 | 28* |
| 2016-10-03 | 2016-09-28 | 5 |
| 2016-11-02 | 2016-11-03 | 1 |
| 2016-11-22 | 2016-11-21 | 1 |
| 2016-12-02 | 2016-12-02 | 0 |

# Method « single-date »

A)

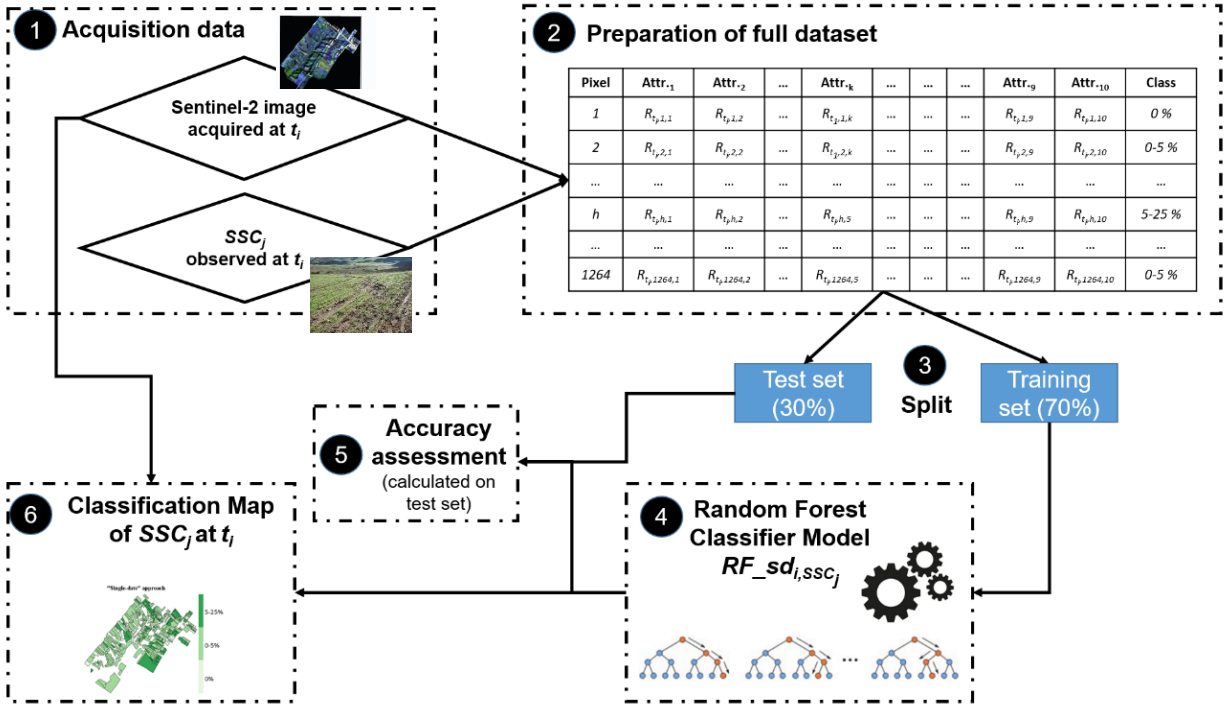


# Method « multi-date »

B)

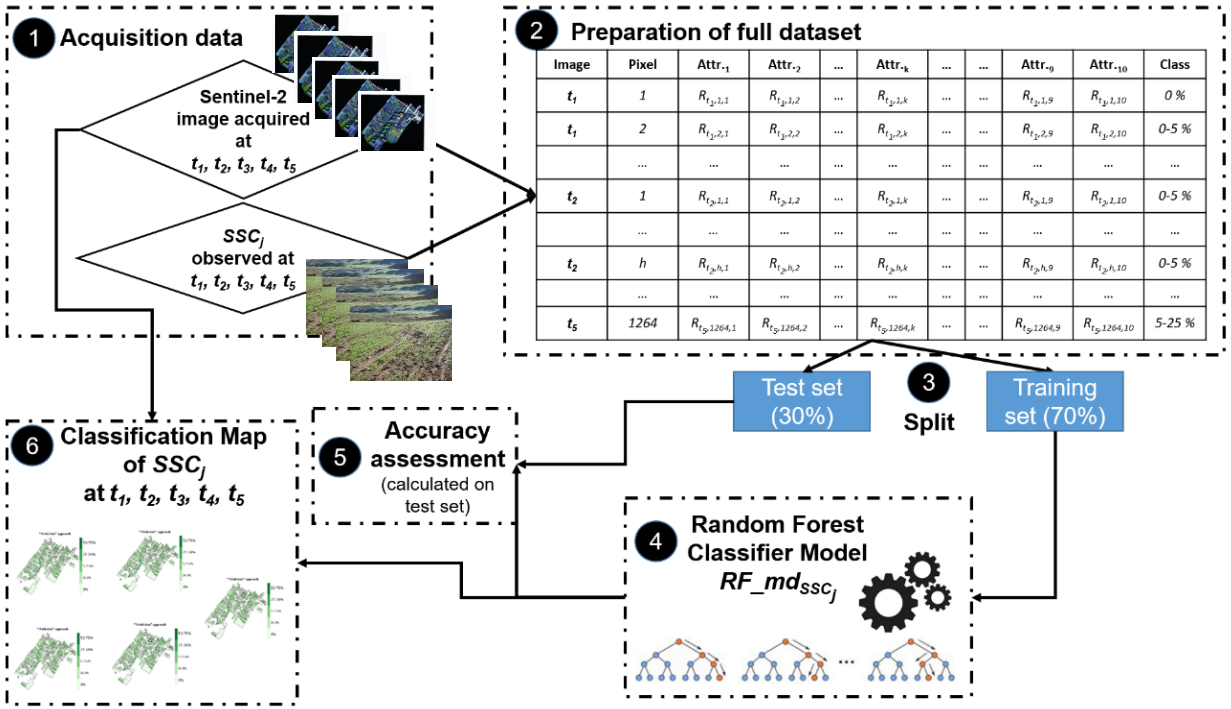

- Both methods provided accurate performances (overall accuracy > 0.79) regardless of the studied *SSC* and the tested Sentinel-2 image

- The “single-date” method did not allow the classification of SSC classes that were not observed on the studied date, while the “multi-date” method allowed the classification of all SSC classes observed in the five Sentinel-2 images

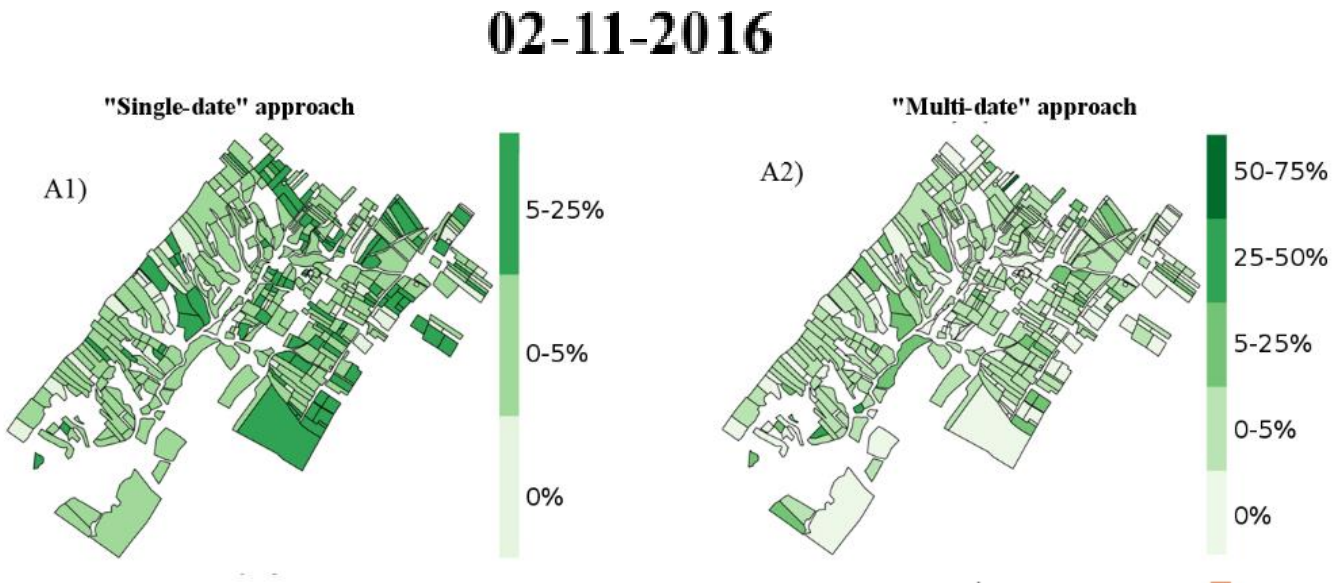


Next question would be : ***Can we estimate the soil infiltration from these soil surface characteristic ?***

Institut de Recherche pour le Développement FRANCE
French National Research Institute for Sustainable Development
CESBIO

## • Climate variability.

o Targets: climate spatiotemporal structures.

o Methodological innovations: disaggregation of climate model simulations using multivariate statistics on various data (in-situ, remote sensing, high resolution meteorological model simulations) or using stochastic weather generator with SAR images.

**-> MetGen stochastic weather generator (PhD N. Fahrani)**

$$\mathbb{P}(WS, AirT, Rh, GR) = \mathbb{P}(WS)\mathbb{P}(AirT|WS)\mathbb{P}(Rh|AirT, WS)\mathbb{P}(Gr|AirT). \quad (1)$$

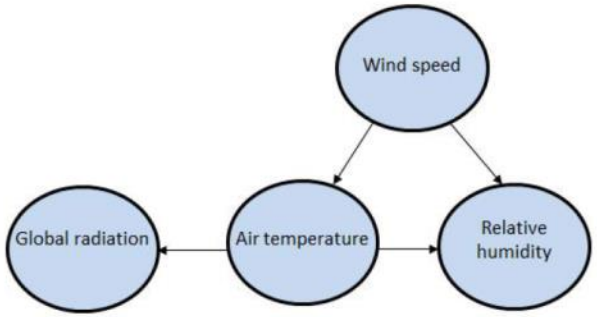


**Figure 4:** *Inter-variable dependency graph yielding the product rule decomposition in (1) which allows to model the dependence structure of the four meteolorogical variables in* `MetGen`.

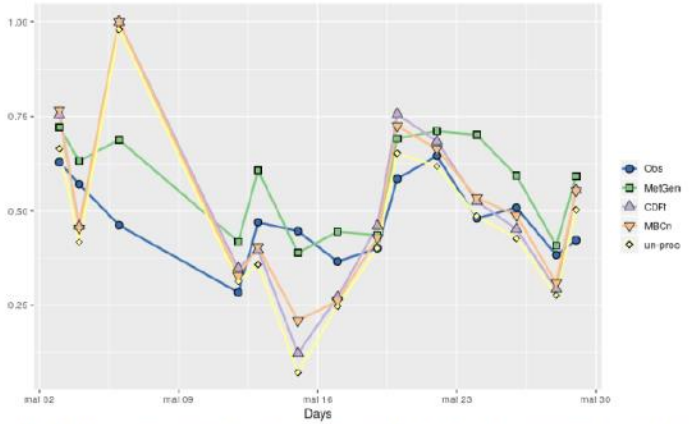


**Figure 12:** *Chronological fluctuations of SI estimates at the satellite overpass times during May 2016 with the different choices of meteorological information (either the observed series or one of the surrogate series) used to constrain the SPARSE energy balance model (see color legend). For* `MetGen`, *a high stress condition series is computed out of the 50 replicated surrogate series.*

**Figure 7:** *Qq-plots for each meteorological variable comparing surrogate series (see color legend) on the y-axis with the observations on the x-axis. Associated Root-Mean-Squared Errors (RMSEs) are indicated in each plot.*

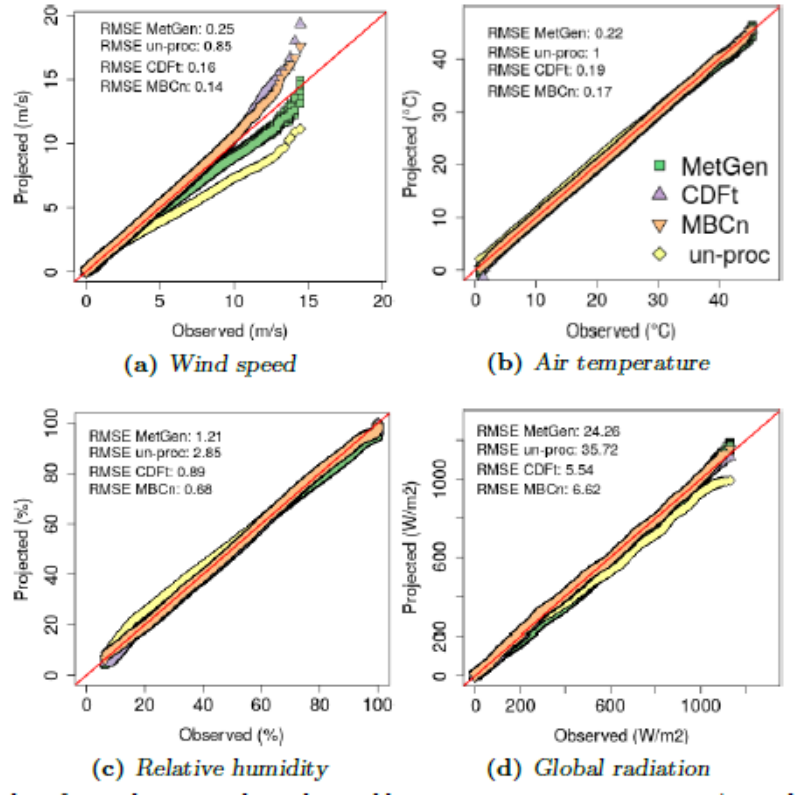

# SAFRAN + ISBA + MEDCORDEX

Moucha et al., MDPI/Atmosphere, 2021

## Evaluation of SAFRAN (2004-2014)

- Regular grid (8 km) versus variable grid

**Mountain station (Aremd)**

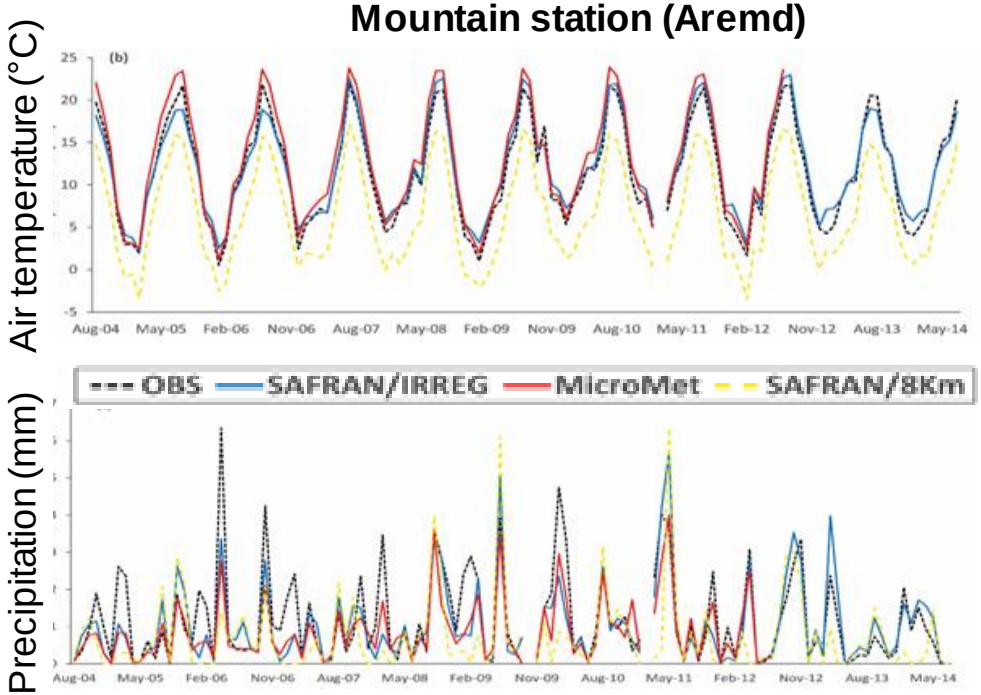


- Rainfall/Snowfall partition

**Tensift catchment**

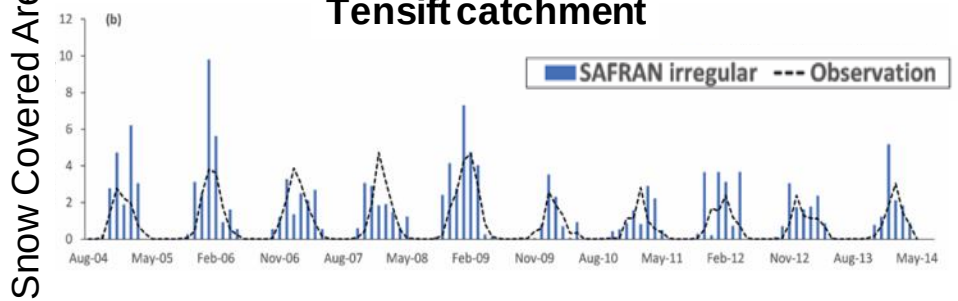


## Futuristic scenarios (2041-2060)

1) Quantile mapping on two stations (plain and mountains)
2) Transfer functions applied to Euro-CORDEX on the Tensift by separating plain and mountainous grid points
3) Compute Delta change on debiased Euro-CORDEX
4) Apply the computed Delta Change to SAFRAN re-analysis

**Air temperature, annual average**

Historical (2004-2014) RCP8.5 (2041-206(

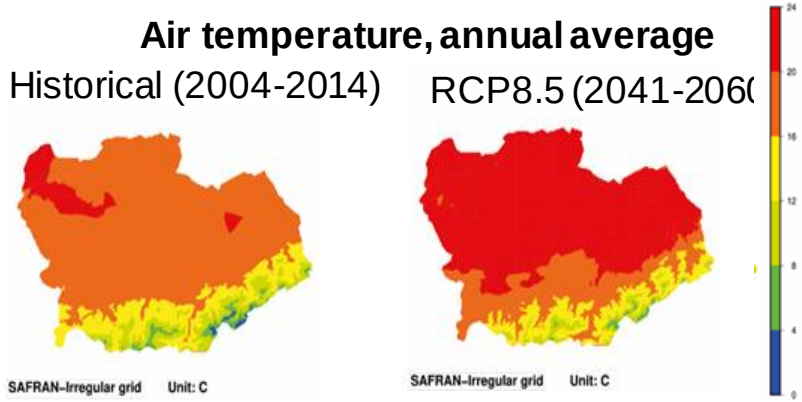


- Stronger warming may be expected during the winter and spring months
- Mountainous areas are expected to face a higher increase in air temperatures than the plains.

UNICA

## Task 1.1: Object geometries and landscape structures

# Activities

Climate variability:

-Disaggregation of climate model simulations using the Multivariate quantile mapping bias Correction and the Principal Component analysis- Collaboration with Julie Careau (LISAH)

UNICA

## Disaggregation of climate model simulations using the Multivariate quantile mapping bias Correction and the Principal Component Analysis- Collaboration with *Julie Careau*

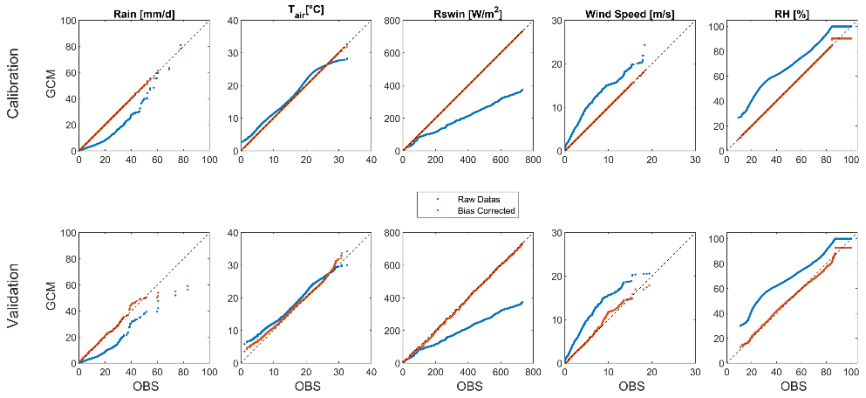


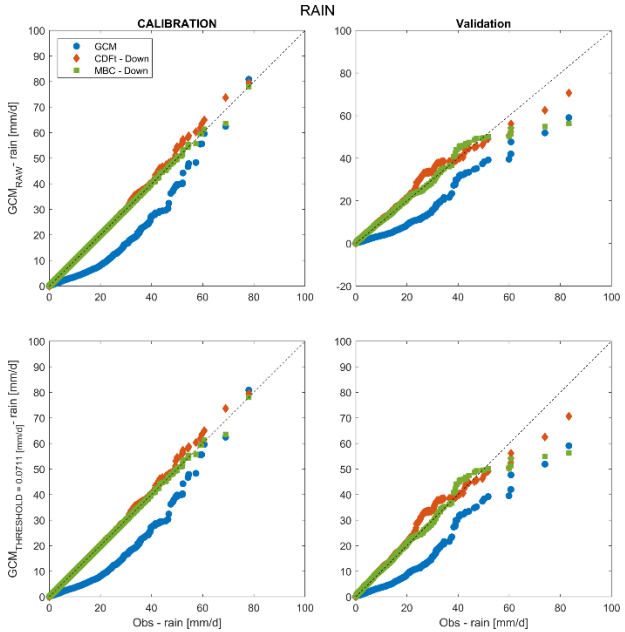


## Estimate of soil moisture in a grass field using Sentinel-1 and Sentinel-2 observations

**Optical and radar products are used for the estimation of soil moisture content using the empirical Change detection method, the semi-empirical Dubois et al. (1995) model, and the physically-based Fung et al. (1992) model**

### *Results from the use of the Dubois model*

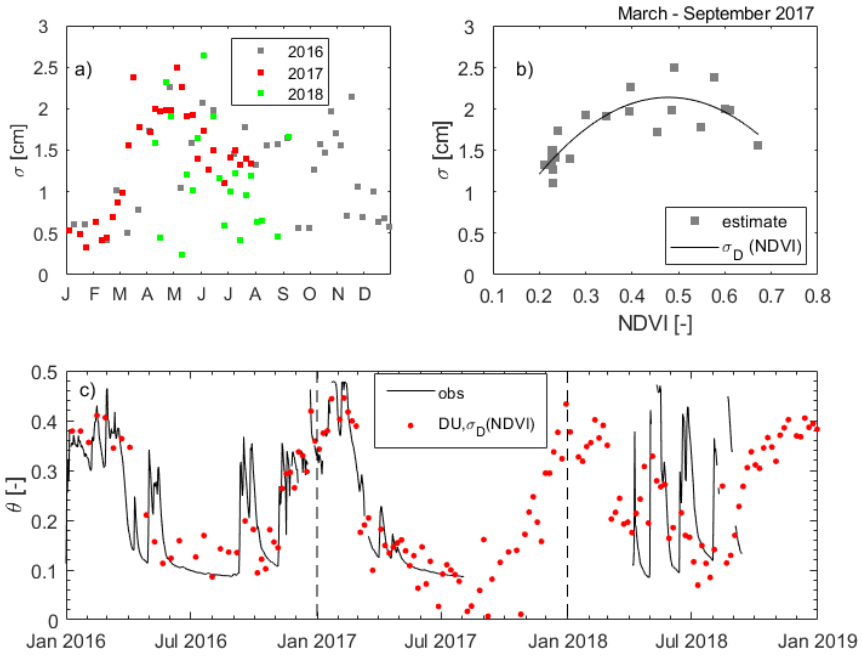

# Task 1.1: object geometries and landscape structures: Climate variability

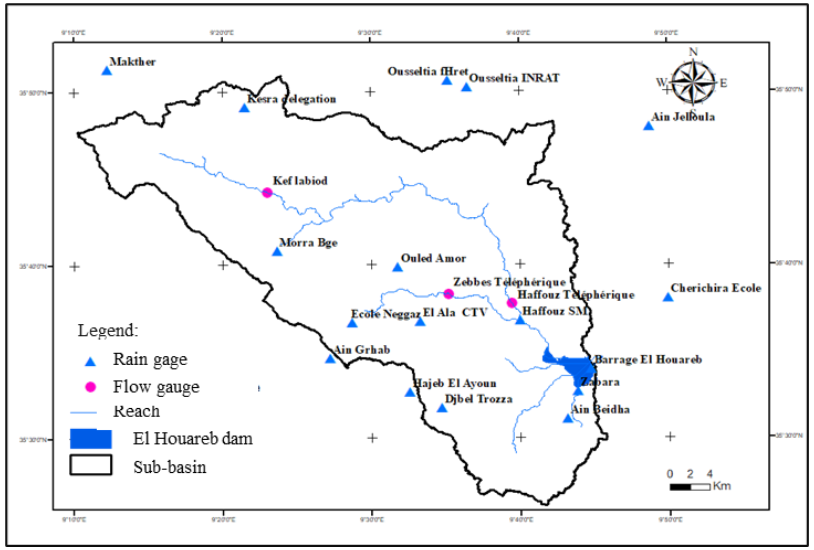


Figure 1 : Rain gage and flow gauge in Merguellil upstream catchment

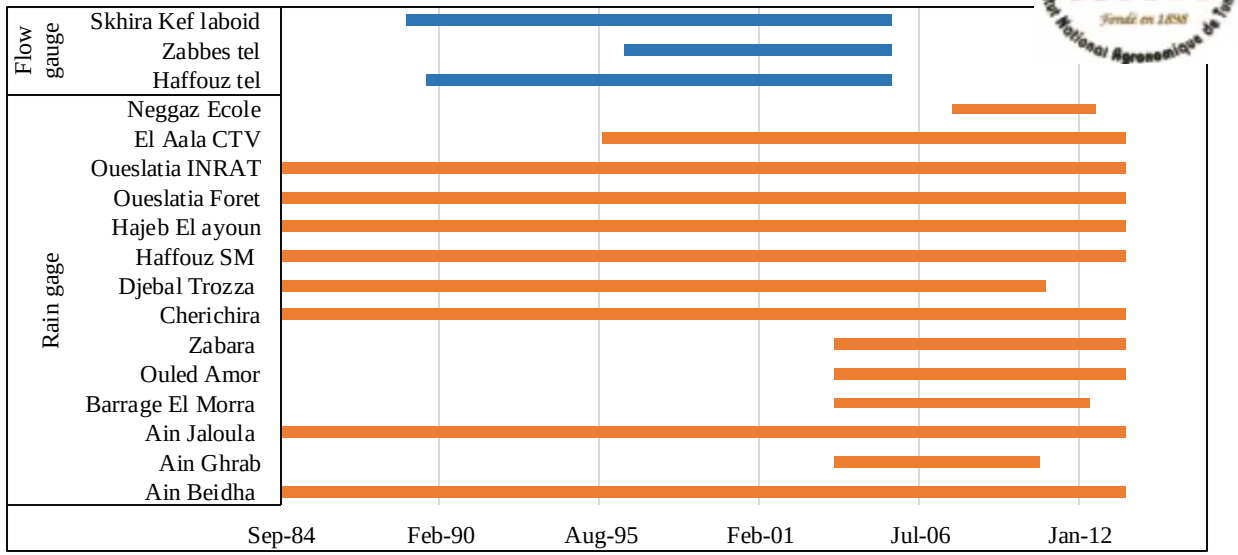


Figure 2: Diagram of rainfall and flow data

## Weather Generator (WGN) : Kairouan

- **The WGN contains the statistical data needed to generate representative daily climate data for the sub-basin.**
- **It can be used to simulate daily climatic data**

| Month | TMPMX | TMPMN | TMPSTDMX | TMPSTDMN | PCPMM | PCPSTD | PCPSKW | PR_W1 | PR_W2 | PCPD | RAINHHMX | SOLARAV | DEWPT | WNDAV |
|---|---|---|---|---|---|---|---|---|---|---|---|---|---|---|
| January | 18.23 | 7.28 | 3.75 | 2.47 | 38.12 | 6.79 | 10.11 | 0.07 | 0.31 | 3.06 | | 9.47 | 8.03 | 2.63 |
| February | 20.65 | 9.06 | 4.39 | 2.89 | 22.42 | 4.23 | 9.15 | 0.08 | 0.27 | 2.65 | | 11.72 | 8.20 | 2.71 |
| March | 24.11 | 11.08 | 4.48 | 2.78 | 26.75 | 5.30 | 14.45 | 0.08 | 0.39 | 3.47 | | 16.07 | 9.85 | 2.72 |
| April | 28.51 | 14.66 | 5.08 | 3.43 | 30.18 | 4.60 | 7.33 | 0.11 | 0.22 | 3.71 | | 18.93 | 11.88 | 2.76 |
| May | 33.77 | 18.70 | 5.27 | 3.44 | 19.66 | 2.79 | 5.63 | 0.06 | 0.26 | 2.53 | | 21.67 | 14.18 | 2.54 |
| June | 36.90 | 21.57 | 3.80 | 2.41 | 10.65 | 1.92 | 7.25 | 0.05 | 0.19 | 1.59 | | 23.83 | 13.72 | 2.54 |
| July | 37.35 | 22.66 | 3.51 | 2.16 | 3.98 | 1.93 | 19.47 | 0.01 | 0.20 | 0.29 | | 25.47 | 14.36 | 2.45 |
| August | 32.72 | 20.41 | 4.24 | 2.40 | 16.45 | 3.13 | 8.87 | 0.06 | 0.15 | 2.00 | | 23.23 | 13.11 | 2.23 |
| September | 28.85 | 17.29 | 4.17 | 3.04 | 42.91 | 5.32 | 5.61 | 0.12 | 0.23 | 4.12 | | 17.91 | 13.33 | 2.25 |
| October | 22.92 | 12.63 | 4.24 | 3.52 | 42.36 | 6.57 | 8.31 | 0.08 | 0.33 | 3.24 | | 13.14 | 9.66 | 2.17 |
| November | 19.14 | 8.62 | 3.43 | 2.95 | 23.29 | 3.70 | 6.90 | 0.07 | 0.29 | 2.65 | | 10.41 | 7.10 | 2.54 |
| December | 17.27 | 6.88 | 3.37 | 2.83 | 32.48 | 5.83 | 8.79 | 0.06 | 0.35 | 2.82 | | 8.27 | 6.18 | 2.64 |

# Task 1.1: object geometries and landscape structures: Climate variability

**Projected (September 2021)**

Extraction of rainfall data from free satellite products (GPM-IMERG and CHIRPS)

Processing of rainfall data (observed and extracted from satellite images) using spatial interpolation methods (R, PYTHON,…)

Develop rainfall indices to study spatial and temporal variability

**issues**

- Scarcity data in arid and semi-arid areas
- difficulty in collecting observed data (not free)

# Task 1.1: Object geometries and landscape structures

- **Deliverable progresses**

- **D1.1.1** [Task 1.1]: dataset @ Month 15 (20) → to be included into project clustered database (WP5).
- **D1.1.2** [Task 1.1]: 2 submitted publications for methodological innovations @ Month 21. DONE !